


## Review

<https://doi.org/10.48130/newcontam-0025-0002>

# A brief review of strobilurin fungicides: environmental exposure, transformation, and toxicity

Zhilei Liu<sup>1,2,3#</sup>, Yuxian Liu<sup>4#</sup>, Henglin Zhang<sup>5</sup>, Yanan Zhao<sup>1,2,3</sup>, Tao Zhang<sup>5</sup>, Yanpeng Cai<sup>1,2,3</sup> and Jingchuan Xue<sup>1,2,3\*</sup> 

Received: 15 June 2025

Revised: 16 July 2025

Accepted: 6 August 2025

Published online: 3 September 2025

## Abstract

Strobilurin fungicides (SFs), a class of quinone outside inhibitor (QoI) agrochemicals, have revolutionized crop protection since their commercialization in the 1990s. This critical review synthesizes global data on environmental distribution, analytical detection methods, toxicological impacts, and environmental transformation of SF. Key findings revealed: (1) SFs residues are ubiquitously detected in agricultural products (e.g., wheat, apples), aquatic systems (median concentration up to 100  $\mu\text{g}\cdot\text{L}^{-1}$ ), and human matrices (e.g., 100% detection of azoxystrobin metabolites in pregnant women's urine); (2) mitochondrial dysfunction emerges as a central toxicity mechanism, with SFs inhibiting complex III activity, reducing ATP synthesis by 28.7%–98.5% in zebrafish embryos, and inducing oxidative stress via ROS overproduction; (3) endocrine disruption and neurotoxic effects were observed at environmentally relevant concentrations (e.g., 1  $\mu\text{g}\cdot\text{L}^{-1}$  trifloxystrobin altered *er* gene expression in medaka); (4) microbial degradation dominated the environmental transformation, showing exceptional catabolic versatility. Despite advancements, critical gaps persist in mixture toxicity assessment, epidemiological correlation, and global biomonitoring. We advocate for integrated approaches combining effect modeling (QSTR/TK-TD), omics technologies, and international surveillance networks to mitigate ecological and health risks in the era of intensifying agrochemical use.

**Keywords:** Strobilurin fungicides, Environmental exposure, Toxicology effect, Transformation

## Highlights

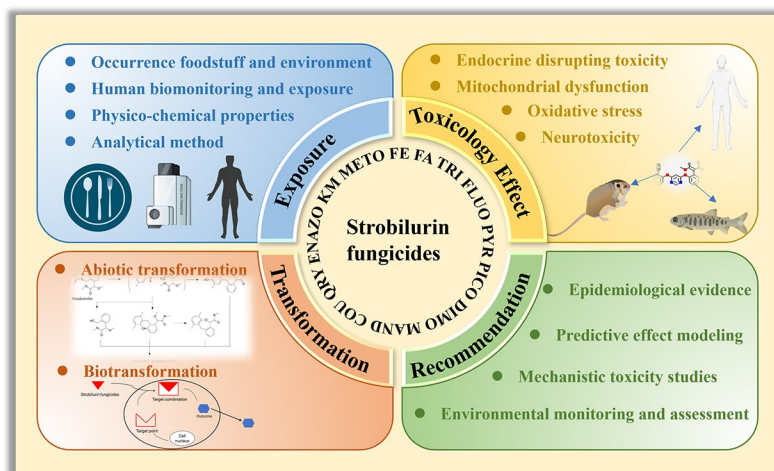
- SF residues are ubiquitous in crops, aquatic systems, and humans, indicating widespread exposure and risks.
- Mitochondrial dysfunction underpins SF toxicity: inhibiting complex III, reducing ATP 28.7%–98.5%, and inducing ROS in zebrafish.
- At environmental levels, SFs trigger endocrine and neurotoxicity, indicating low-dose risks.
- Microbial degradation dominates SF transformation, offering novel remediation insights.

Authors contributed equally: Zhilei Liu and Yuxian Liu

\* Correspondence: Jingchuan Xue ([xue@gdut.edu.cn](mailto:xue@gdut.edu.cn))

Full list of author information is available at the end of the article.

## Graphical abstract



## Introduction

Strobilurin fungicides (SFs), a novel class of fungicides inspired by natural strobilurins, represent a significant advancement in agricultural chemical development<sup>[1]</sup>. Azoxystrobin (AZO), a pioneering commercial SF, was introduced by Syngenta in 1992<sup>[2,3]</sup>. Following its market debut in 1996, the application of AZO rapidly expanded, culminating in its status as the top-selling fungicide globally by 2014. The evolution of SFs continued with the introduction of methoxyiminoacetate derivatives, such as kresoxim-methyl (KM) by BASF in 1992, and trifloxystrobin (TRI) by Bayer in 1998<sup>[2]</sup>. This was followed by a wave of innovation, with industry leaders including Bayer, BASF, Shionogi, DuPont, and Aventis discovering and patenting a multitude of new SFs<sup>[4,5]</sup>; the timeline of these developments is illustrated in Fig. 1.

The widespread adoption of SFs in agricultural practices over several decades can be attributed to their broad-spectrum efficacy, cost-effectiveness, potent germicidal activity, and rapid degradation properties<sup>[6]</sup>. By 2016, SFs had reached the pinnacle of fungicide sales, capturing a significant 20% of the global market share<sup>[7]</sup>. Data from the United States Geological Survey (USGS) reveal that in 2016, the combined application of AZO, pyraclostrobin (PYR), picoxystrobin (PICO), TRI, fluoxystrobin (FLUO), and KM in the United States reached approximately 5.7 million pounds<sup>[8]</sup>. Concurrently, China's usage of these fungicides was estimated at around 10,000 tons (~220 million pounds) in 2018, underscoring the substantial reliance on SFs in major agricultural economies<sup>[9]</sup>.

The widespread application of SFs has led to numerous instances of environmental contamination on a global scale, reflecting their extensive use in agriculture. For example, residues of SFs have been identified in various crops and vegetables across Europe, as well as in wheat in China. Additionally, these compounds have been detected in environmental matrices such as surface water, ground-water, and both indoor and outdoor dust in the United States<sup>[10,11]</sup>. The concentrations of SFs in aquatic systems can exceed 100 µg·L<sup>-1</sup>, posing a potential threat to aquatic biodiversity due to their increasing application in crop protection and subsequent entry into water bodies. Initially perceived as non-toxic to humans, birds, and other mammals, emerging research has revealed that SFs exhibit significant toxicity to aquatic organisms<sup>[5]</sup>. Among these, PYR, AZO, and KM are identified as the most toxic fungicides to aquatic ecosystems<sup>[8]</sup>.

SFs are predominantly utilized as protectants, curative agents, and translaminar fungicides, offering versatile applications in plant

disease management<sup>[12]</sup>. A pivotal factor contributing to the remarkable commercial success of AZO is its broad-spectrum efficacy against fungi from all four major classes of plant pathogens: Ascomycetes, Basidiomycetes, Deuteromycetes, and Oomycetes<sup>[3,12]</sup>. Biochemically, SFs are classified as quinone outside inhibitors (QoI), exerting their fungicidal activity by disrupting energy production within fungal cells, as illustrated in Fig. 1. The (E)-β-methoxyacrylate group, highlighted in red, represents the toxiphoric moiety central to the structure and function of SFs<sup>[12]</sup>. Mechanistically, SFs inhibit electron transfer at the quinol oxidation site (Qo site) of the cytochrome bc1 complex, thereby obstructing adenosine triphosphate (ATP) synthesis<sup>[2]</sup>. Furthermore, this inhibition can result in electron leakage from the mitochondrial respiratory chain, triggering cellular oxidative stress. This oxidative stress is subsequently mitigated by mitochondrial manganese superoxide dismutase (MnSOD), which plays a critical role in detoxification<sup>[13]</sup>.

The ecological risks posed by SFs are of growing concern due to their extensive agricultural application, pervasive environmental occurrence, and unintended ecological consequences stemming from non-target toxicity. Nevertheless, critical knowledge gaps persist regarding their current environmental status, analytical detection methodologies, and toxicological profiles in aquatic and terrestrial ecosystems, while future research priorities remain poorly defined. Thus, in this critical review, we first compiled the occurrence of SFs across various environmental matrices, agricultural crops, and human metabolites, alongside a summary of analytical methodologies for detecting these compounds in diverse sample types. Subsequently, we delved into the toxicological impacts of SFs, encompassing mitochondrial dysfunction, oxidative stress, endocrine-disrupting effects, and neurotoxicity. Furthermore, we explored potential degradation pathways of strobilurin fungicides based on different transformation routes. Conclusively, we identified current research gaps and proposed future directions for exploration, offering recommendations to advance the current state of SF research.

## Environmental exposure

## Physico-chemical properties

The physico-chemical properties and structural characteristics of SFs are summarized in Table 1. Generally, all natural strobilurins share a common methyl (E)-3-methoxy-2-(5-phenylpenta-2,4-dienyl) acrylate

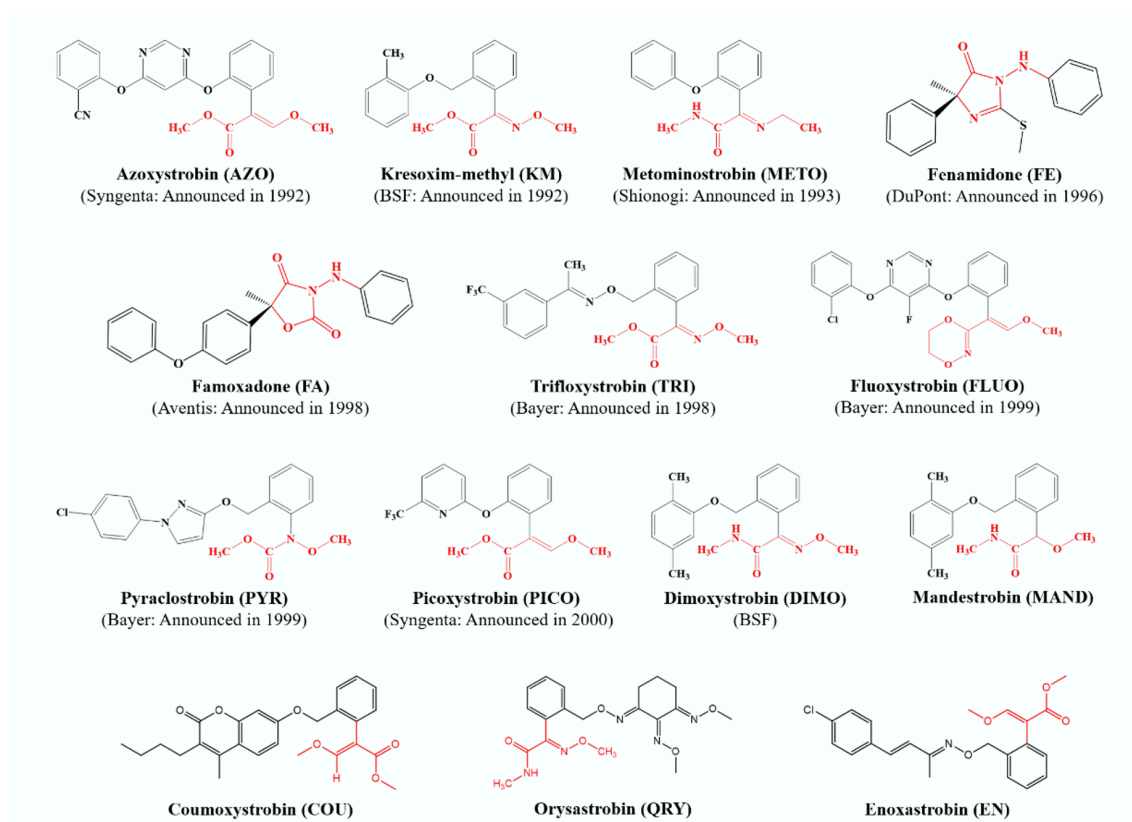


**Fig. 1** Announcement time and chemical structures of 14 strobilurin fungicides.

moiety, with variations primarily occurring in the aromatic ring substitutions at positions 3 and 4. These compounds exhibit relatively complex structures, which introduce multiple metabolic reaction sites, thereby facilitating diverse metabolic pathways.

Most SFs demonstrate moderate to high hydrophilicity, with a median log octanol-water partition coefficient ( $K_{ow}$ ) of 3.59 (Fig. 2). Although their water solubility varies significantly across groups (median log water solubility ranging from  $-0.41$  to  $1.06$ ; Fig. 2), they are frequently detected in aquatic environments. Additionally, SFs generally exhibit moderate adsorption potential to organic carbon, with a median log organic carbon-water coefficient ( $K_{oc}$ ) of 3.35 (Fig. 2). These compounds tend to accumulate in environmental organic phases due to their low volatility, as indicated by a high log octanol-air partition coefficient ( $K_{oa}$ ) of  $10.38$  (Fig. 2). Notably, when  $\log K_{oa} > 8$  and  $\log K_{ow} > 5$ , compounds exhibit low water solubility and are more likely to adsorb to particulate matter in both the atmosphere and water bodies<sup>[14]</sup>, TRI and PYR meet these criteria (Table 1), suggesting their potential for higher concentrations and detection frequencies in atmospheric and aquatic particulate matter. For most aquatic organisms, compounds with  $5 < \log K_{ow} < 8$  exhibit strong bioaccumulation potential<sup>[15]</sup>, TRI and PYR are likely to demonstrate significant bioaccumulation, whereas compounds with  $\log K_{ow} < 5$ , such as AZO, KM, metaminostrobin (METO), fenamidone (FE), FLUO, PICO, dimoxystrobin (DIMO), and mandestrobin (MAND), exhibit higher hydrophilicity and reduced partitioning into lipid tissues, resulting in lower bioaccumulation potential (Table 1). In contrast to aquatic organisms, compounds with  $2 < \log K_{ow} < 5$  and  $\log K_{oa} > 6$  can still achieve bioaccumulation in atmospheric media through respiratory uptake<sup>[15]</sup>, and METO and famoxadone (FA) may utilize this pathway for accumulation.

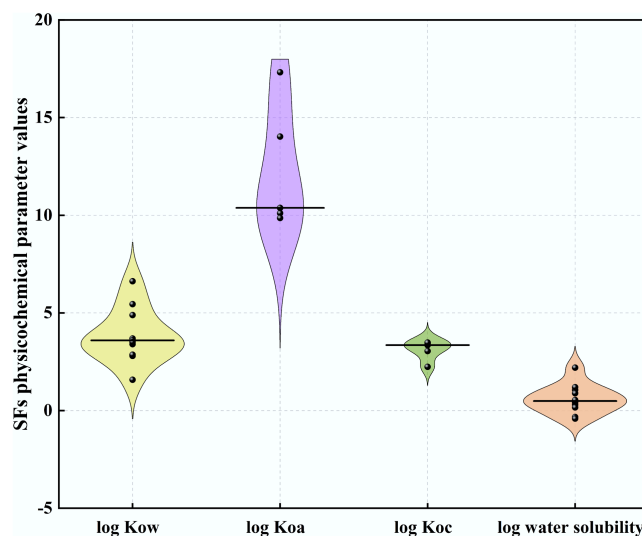


**Fig. 2** Violin plots of physico-chemical properties related to mobility and dissipation for strobilurins fungicides currently registered for use in the EU (log  $K_{ow}$ :  $n = 11$ , log  $K_{oa}$ :  $n = 5$ , log  $K_{oc}$ :  $n = 5$ , log water solubility ( $20^\circ\text{C}$ ):  $n = 5$ ). Black bars within violins represent medians.

## Analytical method

SFs were initially introduced for agricultural use, but their widespread application has led to the detection of SF residues in both environmental and biological systems. While early concerns focused on residues in agricultural soils and crops, recent attention has shifted to the potential toxicity of SFs to aquatic ecosystems and human

**Table 1** Physico-chemical properties and structural characteristics of strobilurin fungicides

Compound	Abbreviation	Structure	Molecular formula	CAS	M.W.	Log K <sub>ow</sub>	Log K <sub>oa</sub>	Log K <sub>oc</sub>	Solubility in water (mg L <sup>-1</sup> ) at 20 °C
Azoxystrobin	AZO		C <sub>22</sub> H <sub>17</sub> N <sub>3</sub> O <sub>5</sub>	131860-33-8	403.40	1.58	14.03	3.05	11.61
Kresoxim-methyl	KM		C <sub>18</sub> H <sub>19</sub> NO <sub>4</sub>	143390-89-0	313.40	3.40	—	—	2.00
Pyraclostrobin	PYR		C <sub>19</sub> H <sub>18</sub> ClN <sub>3</sub> O <sub>4</sub>	175013-18-0	387.80	5.45	17.32	3.48	1.43
Trifloxystrobin	TRI		C <sub>20</sub> H <sub>19</sub> F <sub>3</sub> N <sub>2</sub> O <sub>4</sub>	141517-21-7	408.40	6.62	9.86	3.35	0.39
Fluoxystrobin	FLUO		C <sub>21</sub> H <sub>16</sub> ClFNO <sub>5</sub>	361377-29-9	458.80	2.86	—	—	2.56
Picoxystrobin	PICO		C <sub>18</sub> H <sub>16</sub> F <sub>3</sub> NO <sub>4</sub>	117428-22-5	367.30	3.60	—	—	3.10
Dimoxystrobin	DIMO		C <sub>19</sub> H <sub>22</sub> N <sub>2</sub> O <sub>3</sub>	149961-52-4	326.40	3.59	—	—	3.50
Metominostrobin	METO		C <sub>16</sub> H <sub>16</sub> N <sub>2</sub> O <sub>3</sub>	133408-50-1	284.30	3.69	10.11	2.24	158.00
Mandestrobin	MAND		C <sub>19</sub> H <sub>23</sub> NO <sub>3</sub>	173662-97-0	313.40	3.51	—	—	15.80
Fenamidone	FE		C <sub>17</sub> H <sub>17</sub> N <sub>3</sub> OS	161326-34-7	311.40	2.80	—	—	7.80
Famoxadone	FA		C <sub>22</sub> H <sub>18</sub> N <sub>2</sub> O <sub>4</sub>	131807-57-3	374.40	4.89	10.38	3.45	0.47

health<sup>[16]</sup>. This review synthesizes the literature on the occurrence of SFs, with agricultural products such as crops, beans, fruits, vegetables, and grape wine being the most commonly analyzed for SF concentrations. Environmental monitoring has primarily targeted soil, surface water, and indoor/outdoor dust, while human and biological sample analyses are increasingly being developed (Table 2).

For the analysis of SFs residues in foodstuffs, including fruits and vegetables, the QuEChERS (Quick, Easy, Cheap, Effective, Rugged, and Safe) method is widely employed as a pretreatment technique,

typically using acetonitrile (ACN) as the extraction solvent<sup>[17–24]</sup>. Additional sample preparation methods, such as liquid-liquid micro-extraction (LLME) and solid-phase extraction (SPE), have also been utilized, with various organic solvents tailored to specific sample types. In environmental matrices, a magnetic SPE extraction method coupled with high-performance liquid chromatography-tandem mass spectrometry (HPLC-MS/MS) has been developed for detecting AZO, oryastrobin (ORY), PICO, DIMO, and KM in lake and tap water. This method has been demonstrated to be simple, time-

**Table 2** Extraction, purification, and analytical methods of strobilurin fungicides

Matrix	Target SFs	Sample preparation	Analytical technique	Recovery (RSD)	LOQ	Ref.
Vegetable, fruit, and food						
Bean	AZO, KM, TRI, DIMO, FLUO, PICO, PYR	LLME (ACN/H <sub>2</sub> O 9:1 <sup>b</sup> )	HPLC/UV-AD	61.6%–98.8% (< 10%)	0.004–0.005 mg·kg <sup>-1</sup>	[34]
Rice	ORY	LLME (DCM/n-Hexane 20:80) Florisil Column Chromatography (EA/DCM 10:90)	HPLC-UV LC-MS/MS	83.9%–92.3% 80.6%–114.8%	0.02 mg·kg <sup>-1</sup> 0.002 mg·kg <sup>-1</sup>	[35]
Apple, grape, wheat	AZO, KM, TRI	Extracted: EA/Cyclohexane Clean-up: GPC	GC-EC GC-NP GC-MS	70%–114%	— <sup>a</sup>	[36]
Pomegranate	AZO, PYR	d-SPE (ACN)	LC-MS/MS	78.7%–98% (< 20%)	0.005 mg·kg <sup>-1</sup>	[17]
Pepper	PYR, PICO	QuEChERS (ACN)	UPLC-MS/MS	91%–107% (3.7%–9.6%)	0.12–0.61 µg·kg <sup>-1</sup>	[21]
Watermelon	FA	LLExtraction: DCM Clean-up: Acetone/petroleum 1:9)	HPLC-UVD	84.91%–99.41% (0.06%–4.93%)	—	[37]
Cucumber	PYR	QuEChERS	UHPLC-MS/MS	89.8%–103.6% (3.6%–7.5%)	8.1 µg·kg <sup>-1</sup>	[18]
Grape, must, wine	AZO	SPE (MeOH) SPE (DCM)	PIF-FI-SPS	84.0%–87.6%, 95.5%–105.9%, 98.5%–111.2%	21 µg·kg <sup>-1</sup> 18 µg·L <sup>-1</sup> 8 µg·L <sup>-1</sup>	[31]
Jujube	PYR, AZO	QuEChERS (ACN)	LC-MS/MS	87.5%–116.2% (3.2%–14.7%)	0.01–0.2 mg·kg <sup>-1</sup>	[24]
Watermelon	TRI	QuEChERS (ACN)	GC-MS/MS	78.59%–92.66%	0.01 mg·kg <sup>-1</sup>	[23]
Apple tree bark	PYR	QuEChERS (ACN-Ammonia)	HPLC-VWD	86.1%–101.4%	0.028–0.080 mg·kg <sup>-1</sup>	[20]
Green bean, pea	AZO	LLME (ACN)	HPLC-UV GC-MS	81.99%–107.85% ( < 20%) 76.29%–100.91% ( < 20%)	0.1 mg·kg <sup>-1</sup>	[38]
Banana	AZO	QuEChERS-Citrate (ACN)	GC-SQ/MS	—	0.022–0.199 mg·kg <sup>-1</sup>	[19]
Pomegranate	AZO, PYR	QuEChERS (ACN); d-SPE (n-Hexane /acetone 9:1)	LC-MS/MS GC-MS	78.7%–98% (< 20%)	0.005 mg·kg <sup>-1</sup> 0.01 mg·kg <sup>-1</sup>	[17]
Water, juice, wine, vinegar	PICO, PYR, TRI	d-LLME (DES: thymol, octanoic acid)	HPLC	77.4%–106.9% (0.2%–6.8%)	—	[39]
Rice	TRI	Extraction solvent (ACN)	LC-MS/MS	74.3%–103.0% (0.5%–6.8%)	—	[40]
Cereal	AZO, PYR, TRI	d-LLME-SFOD (Nonanoic acid)	HPLC-MS/MS	82.0%–93.2% (1.6%–7.4%)	—	[41]
Apple, citrus, cucumber, potato, tomato	AZO, KM, PYR	—	Electrokinetic capillary chromatography	81.7%–96.1% 86.5%–95.7% 87.3%–97.4%	0.005–2.5 mg·kg <sup>-1</sup>	[32]
Tea	TRI	QuEChERS	GC-MS	80.7%–105.8% (<9.3%)	0.05 mg·kg <sup>-1</sup>	[22]
Red wine	TRI, KM, PICO	Cross-linked poly as a sorbent	FPIAs-monoclonal antibodies	80%–104% (<12%)	—	[33]
Cotton seed	TRI, PICO, KM, AZO	d-LLME (ACN)	GC-ECD	87.7%–95.2% (4.1%–8.5%)	—	[42]
Grape wine	AZO, KM, TRI, PYR, FA, FE	LLME (EA/n-Hexane 50:50)	LC-ADA GC-MS	95.5% ± 5% 104% ± 6%	0.3–0.6 mg·L <sup>-1</sup> 0.4–0.8 mg·L <sup>-1</sup>	[43]
Environmental media						
Lake, river, tap water	AZO, ORY, PICO, DIMO, KM	Magnetic SPE	HPLC-MS/MS	80.8%–109%	0.18–0.24 mg·L <sup>-1</sup>	[25]
Soil, water,	FA	SPE (ACN)	UHPLC-Orbitrap-MS	70%–120% (< 20%)	0.1 mg·kg <sup>-1</sup> 1 µg·L <sup>-1</sup>	[44]
Atmosphere	AZO, DIMO, FLUO, KM, PYR, TRI	—	LC-MS/MS	91.6% ± 12.2% 99.9% ± 5.6% 100.8% ± 10.4% 101.2% ± 0.2% 99.9% ± 0.7% 97.7% ± 6.3%	—	[45]
Biological Sample						
Fish gill, blood, liver, muscle,	PYR	Mixtures of PSA, C <sub>18</sub> , MgSO <sub>4</sub> QuEChERS-PC Waters Oasis HLB SPE	UPLC-MS/MS	112.5%–276.2% ( < 10%) 45.3%–259.7% ( < 10%) 86.94%–229.9% ( < 10%)	0.002 mg·kg <sup>-1</sup>	[26]
Human urine	AZO, PYR	d-LLME (Choline chloride / sesamol 1:3)	HPLC-MS/MS	50%–101%	0.03–0.07 ng·mL <sup>-1</sup>	[28]
Human urine	AZO	SPE (ACN)	UHPLC-Orbitrap-MS	90%–103%	0.01 ng·mL <sup>-1</sup>	
Human blood	AZO, FA	SPE (Dichloromethane / methanol 9:1)	GC-MS/MS	70%–120% (< 20%)	< 1.45 ng·mL <sup>-1</sup>	[30]

(to be continued)



**Table 2** (continued)

Matrix	Target SFs	Sample preparation	Analytical technique	Recovery (RSD)	LOQ	Ref.
Indoor dust						
New dry wall, gypsum, house dust	AZO, PYR, TRI, FLUO	Extracted: DACM/Hexane, 1:1 Clean-up: ENVI-Florisil	LC-MS/MS	92%–96% 73% 36% 38%	–	[11]
Indoor dust	AZO, FLUO, TRI, PYR	Extracted: ACN Clean-up: ENVI-Florisil	UHPLC-MS/MS	91.2%–108%	0.005–0.01 ng·mL <sup>-1</sup>	[46]

<sup>a</sup>: '–' indicates that the sample preparation method or recovery data were not recorded in the related literature. <sup>b</sup>: Extraction solvent ratio, indicated by the volume ratio. Abbreviation: d-LLME (Dispersive Liquid-Liquid Microextraction), d-SPE (Dispersive Solid Phase Extraction), GPC (Gel Permeation Chromatography), DES (Deep Eutectic Solvents), SFOD (Solidification floating organic droplets), ACN (Acetonitrile), DCM (Dichloromethane).

efficient, and highly sensitive<sup>[25]</sup>. Research on SFs residue analysis in biological samples remains limited, with pretreatment methods largely mirroring those used for environmental and agricultural samples<sup>[26–30]</sup>.

Instrumental analysis of SFs has predominantly relied on liquid chromatography (LC) and gas chromatography (GC) coupled with tandem mass spectrometry (MS/MS). In 2007, Flores et al. pioneered the determination of AZO residues in grapes, must, and wine using a multicommuted flow injection-solid phase spectroscopy (FI-SPS) system combined with photochemically induced fluorescence (PIF)<sup>[31]</sup>. Guo et al. advanced the field by developing a nonaqueous micellar electrokinetic capillary chromatography method with indirect laser-induced fluorescence (LIF), offering advantages such as low solvent consumption, rapid analysis, and high separation efficiency. This method achieved limits of quantification (LOQs) of 0.001 mg·kg<sup>-1</sup> for AZO, KM, and PYR, significantly lower than those obtained by traditional HPLC-MS or GC-MS<sup>[32]</sup>. Additionally, fluorescence polarization immunoassays (FPIAs) based on monoclonal antibodies have been optimized for the detection of SFs in vegetables and fruits, providing a sensitive and specific analytical approach<sup>[33]</sup>.

## Occurrence in foodstuffs and the environment

### Foodstuffs

SFs are extensively utilized in agricultural practices, with residues reported in staple crops such as wheat, rice, cucumbers, apples, and grapes across regions including China, Brazil, the United States, and Europe (Table 3). Among these, AZO exhibits the highest detection frequency, likely attributable to its early commercialization and widespread adoption. Notably, the highest concentrations of AZO have been documented in wheat, whereas TRI shows the lowest levels. Research on SFs residues in foodstuffs predominantly appears in food science journals, focusing on the development and validation of analytical methods, as well as the assessment of environmental residue concentrations.

### Environment

Owing to their broad application in crop disease management, SFs residues were initially reported in agricultural soils, followed by detections in surface water, drinking water, sediments, and indoor dust (Table 3). Compounds such as AZO, FLUO, PYR, and TRI are frequently detected across environmental matrices, demonstrating seasonal fluctuations characterized by elevated concentrations in summer and reduced levels in winter. This pattern aligns with agricultural application cycles, where fungicide use peaks during warmer months. Furthermore, SF concentrations in soils and sediments typically exceed those in aquatic systems, a phenomenon driven by their moderate adsorption potential to organic carbon (median log  $K_{oc}$  for SFs: 3.35), which promotes hydrophobic partitioning into organic-rich environmental phases<sup>[25, 47–50]</sup>.

**Table 3** Concentrations of strobilurin fungicides in foodstuffs and environmental media

Matrix	Target SFs	Concentration	Region	Ref.
Foodstuff				
Wheat	PYR	0.08–9.91 mg·kg <sup>-1</sup>	China	[51]
Ginseng root, Ginseng stem and leaf	AZO	0.343–9.40 mg·kg <sup>-1</sup>	China	[52]
Pepper	PYR	1.68–3.27 mg·kg <sup>-1</sup>	China	[21]
	PICO	2.79–2.80 mg·kg <sup>-1</sup>		
Coffee bean	AZO	< 1.43 µg·kg <sup>-1</sup>	Brazil	[34]
	DIMO	< 1.46 µg·kg <sup>-1</sup>		
	KM	< 1.48 µg·kg <sup>-1</sup>		
	PICO	< 1.33 µg·kg <sup>-1</sup>		
	TRI	< 1.54 µg·kg <sup>-1</sup>		
Watermelon leaf	Fa	19.695 mg·kg <sup>-1</sup>	China	[37]
Banana	AZ	0.05–2.0 mg·kg <sup>-1</sup>	Brazil	[19]
Corn	AZO	0.01–0.024 mg·kg <sup>-1</sup>	China	[53]
	TRI	< LOQ		
	PYR	0.013–0.065 mg·kg <sup>-1</sup>		
Apple	PYR	0.01–0.070 mg·kg <sup>-1</sup>	China	[54]
Dried grape	PYR	0.01–0.024 mg·kg <sup>-1</sup>	Turkey	[55]
Dried apricot	TRI	0.01–0.162 mg·kg <sup>-1</sup>		
Environment				
Soil	AZO	0.726 mg·kg <sup>-1</sup>	China	[52]
Soil	AZO	8.9–15.7 µg·kg <sup>-1</sup>	Vietnam	[56]
Sediment		5.5–35.0 µg·kg <sup>-1</sup>		
Drinking water	AZO	0.37–3.66 ng·L <sup>-1</sup>	China	[50]
	FLUO	< MDL ~0.011 ng·L <sup>-1</sup>		
	PYR	0.01–0.25 ng·L <sup>-1</sup>		
	TRI	0.07–1.03 ng·L <sup>-1</sup>		
Suspended solid	AZO	0.02–0.01 ng·L <sup>-1</sup>	China	[50]
	FLUO	< MDL		
	PYR	0.04–0.48 ng·L <sup>-1</sup>		
	TRI	< MDL ~ 0.007 ng·L <sup>-1</sup>		
Drinking water	AZO	0.036–2.41 µg·L <sup>-1</sup>	Vietnam	[57]
	TRI	0.003–0.56 µg·L <sup>-1</sup>		
Stream	AZO	0.008–1.13 µg·L <sup>-1</sup>	the United States	[58]
	PYR	0.006–0.054 µg·L <sup>-1</sup>		
Groundwater	AZO	0.2–0.9 ng·L <sup>-1</sup>	the United States	[49]
	PYR	0.1–4.8 ng·L <sup>-1</sup>		
Surface water	AZO	30.6–59.8 ng·L <sup>-1</sup>	the United States	[49]
	PYR	15.2–239 ng·L <sup>-1</sup>		
Surface water	AZO	0.01–47.3 ng·L <sup>-1</sup>	China	[59]
	FLUO	< MDL ~0.10 ng·L <sup>-1</sup>		
	PYR	0.01–0.52 ng·L <sup>-1</sup>		
	TRI	< MDL ~0.21 ng·L <sup>-1</sup>		
Indoor dust	AZO	< MDL ~21.9 ng·g <sup>-1</sup>	China	[46]
	FLUO	< MDL ~1.91 ng·g <sup>-1</sup>		
	PYR	< MDL ~1,946 ng·g <sup>-1</sup>		
	TRI	< MDL ~9.52 ng·g <sup>-1</sup>		

## Human biomonitoring

Concerns regarding the potential health risks of SFs to humans have grown in recent years. However, research on SF residues in human matrices remains limited, with only a small number of studies reporting detectable concentrations to date.

### Widespread exposure in sensitive populations

Jamin et al. pioneered the identification of AZO metabolites in urine samples from 3,421 pregnant women in France<sup>[60]</sup>. In 2010, AZO and FA were detected in blood samples from pregnant women in China, with mean concentrations (detection rates) of 0.08 ng·mL<sup>-1</sup> (3%) and 0.27 ng·mL<sup>-1</sup> (23%), respectively<sup>[30]</sup>. Hu et al. reported AZO exposure (measured as AZ-acid) in 100% of urine samples from pregnant women and 70% of samples from children, with median levels of 0.10 and 0.07 ng·mL<sup>-1</sup>, respectively. The average estimated daily intake (EDI) was 75.6 ng·kg<sup>-1</sup>·d<sup>-1</sup> for pregnant women, and 112.6 ng·kg<sup>-1</sup>·d<sup>-1</sup> for children<sup>[29]</sup>.

### Limited detection in healthy volunteers

Gallo et al. analyzed urine samples from 10 healthy volunteers, detecting AZO (0.03 µg·g<sup>-1</sup> creatinine), and PYR (0.03 µg·g<sup>-1</sup> creatinine) in only one individual<sup>[28]</sup>.

## Toxicology effect

### Mitochondrial dysfunction

#### Aquatic species studies

SFs function by inhibiting ATP synthesis and disrupting fungal energy metabolism. However, growing evidence highlights their unintended mitochondrial toxicity in non-target aquatic organisms. Mitochondrial dysfunction is typically quantified through oxygen consumption rate (OCR) measurements, including basal respiration, oligomycin-sensitive ATP-linked respiration, FCCP-uncoupled maximal respiration, and non-mitochondrial oxygen consumption<sup>[61]</sup>.

#### Mitochondrial respiration inhibition

In zebrafish embryos, Yang et al. demonstrated that lethal concentrations of PYR (486 µg·L<sup>-1</sup>), TRI (403 µg·L<sup>-1</sup>), and AZO (408 µg·L<sup>-1</sup>) reduced OCR by 98.5%, 73.1%, and 28.7%, respectively, indicating potent suppression of both mitochondrial and non-mitochondrial respiration<sup>[62]</sup>. Even sublethal PYR exposure (100 µg·L<sup>-1</sup>) significantly diminished basal respiration and non-mitochondrial OCR in embryos<sup>[9]</sup>.

#### Impairment of mitochondrial complexes and energy metabolism

Exposure to 10–20 µg·L<sup>-1</sup> AZO or PYR in zebrafish larvae markedly reduced activities of mitochondrial complex III (ubiquinol-cytochrome c reductase) and complex IV (cytochrome c oxidase), coupled with diminished ATP content<sup>[63,64]</sup>. Cao et al. directly visualized mitochondrial ultrastructural damage, including membrane degradation, rupture, and swelling, in zebrafish liver tissues following 8-d AZO exposure (10 µg·L<sup>-1</sup>). Notably, larval zebrafish exhibited greater susceptibility to AZO-induced mitochondrial dysfunction than adults, accompanied by downregulated *Cytb* transcription<sup>[63]</sup>.

#### Transcriptomic and histopathological effects

Transcriptomic profiling of zebrafish exposed to TRI, KM, AZO, or PYR during early developmental stages revealed significant perturbations in pathways associated with apoptosis, carcinogenesis, organelle membranes, and mitochondrial integrity<sup>[65]</sup>. In fish, gills serve as primary sites for pollutant uptake; acute PYR exposure (500 µg·L<sup>-1</sup>) induced severe histopathological lesions, mitochondrial dysfunction, energy depletion, and respiratory impairment in gill tissues<sup>[66]</sup>.

#### Toxicity in algal systems

Liu et al.<sup>[67]</sup> demonstrated that KM, PYR, TRI, and PICO at environmentally relevant concentrations (10–50 µg·L<sup>-1</sup>) inhibited *bc<sub>1</sub>*

complex activity in *Chlorella vulgaris*, impairing photosynthetic efficiency. Comet assays further revealed DNA damage in algal cells, suggesting genotoxic risks posed by SFs in aquatic ecosystems<sup>[7]</sup>.

### Mammalian studies

AZO has been shown to dose-dependently inhibit cellular respiration by targeting the quinol oxidation (Qo) site of mitochondrial complex III in rat liver. Interestingly, AZO also demonstrated systemic benefits in regulating glucose and lipid homeostasis in high-fat diet-fed mice, suggesting a dual role in metabolic modulation<sup>[68]</sup>.

### Mitochondrial dysfunction and toxicity

Exposure to KM at concentrations below the Acceptable Daily Intake (ADI) induced mitochondrial dysfunction in fibroblast-like renal Vero cells, characterized by elevated mitochondrial superoxide production and reduced mitochondrial transmembrane potential<sup>[69]</sup>. Similarly, Jang et al. investigated the effects of TRI on human skin keratinocytes (HaCaT cells) at the organelle level, revealing that mitochondrial damage and mitophagy contribute to keratinocyte toxicity. These findings suggest a potential mechanistic link between TRI exposure and the development of skin diseases (Table 4)<sup>[70]</sup>.

### Anticancer potential of AZO

Beyond its environmental and toxicological implications, AZO has shown promise as a potential chemotherapeutic agent. Studies have demonstrated that AZO induces apoptosis in cancer cells, including esophageal squamous cell carcinoma (KYSE-150)<sup>[71,72]</sup>, and hepatocellular carcinoma (HepG2)<sup>[68,73]</sup>, through activation of the mitochondrial apoptotic pathway. This highlights the potential for repurposing AZO as a therapeutic agent in oncology.

### Oxidative stress

Accumulating evidence has demonstrated that exposure to SFs can induce oxidative stress in biological organisms. PYR has been shown to disrupt oxidative balance in earthworms, primarily characterized by a dose-dependent increase in reactive oxygen species (ROS) levels. This elevation in ROS can impair the antioxidant defense system, ultimately leading to DNA damage<sup>[74]</sup>. Similarly, TRI, AZO, and KM have been reported to alter antioxidant enzyme activities, including increased catalase (CAT) and peroxidase (POD) activities and decreased superoxide dismutase (SOD) activity. These changes weaken the oxidative defense system and exacerbate oxidative stress, resulting in developmental impairments. Additionally, exposure to these SFs downregulated the expression of growth-related genes such as IGF-1, IGF-2, and GHR, leading to abnormal growth and developmental malformations<sup>[67]</sup>. Cao et al. investigated the effects of AZO exposure on maternal zebrafish and their offspring, revealing that maternal toxicity influenced the expression of oxidative stress-related genes in embryos. Furthermore, offspring exposed to the same environment exhibited more severe oxidative stress responses, highlighting the potential for transgenerational impacts of SFs on aquatic organisms<sup>[75]</sup>.

### Endocrine-disrupting toxicity

SFs, including TRI, KM, PYR, and AZO, have demonstrated significant detrimental effects on the development and reproduction of aquatic species such as medaka, *D. magna*, and zebrafish. These substances act as potential endocrine disruptors and induce various developmental malformations.

### Reproductive effects

Exposure to TRI disrupts the sex hormone pathway and xenobiotic metabolism in medaka, significantly up-regulating the mRNA levels of the *er* gene at concentrations above 1 µg·L<sup>-1</sup>. This disruption adversely affects embryonic and larval development<sup>[76]</sup>. The reproduction of *D. magna* is significantly affected by the three SFs (KM, PYR, and TRI). Increased concentrations of these fungicides result in reduced brood

numbers per female and decreased fecundity, with females showing particularly high sensitivity<sup>[77]</sup>.

### Transcriptomic alterations

Exposure to SFs results in the up-regulation of genes related to apoptosis, disease infection, and cancer pathways<sup>[65]</sup>.

### Lethal and teratogenic effects

Although high concentrations of TFS, KM, AZO, and PYR do not cause embryonic mortality in zebrafish, they lead to developmental issues such as reduced hatching rates, pericardial edema, decreased heart rates, and impaired metabolic cycles<sup>[6,8,16,67]</sup>. According to Wu et al., exposure to PYR, TRI, and AZO induces lethal and teratogenic effects, with affected embryos exhibiting microcephaly, hypopigmentation, somite segmentation, and narrow fins. These effects are consistent across single and combined exposures, displaying a strong synergistic interaction that enhances malformation rates in a concentration-dependent manner<sup>[78]</sup>.

### Neurotoxicity

Few studies were focused on the neurotoxicity of SFs, but certain evidence proved that PYR, TRI, FA, and FE might induce transcriptional changes *in vitro*, which were similar to those seen in brain samples from humans with autism, Alzheimer's disease, and Huntington's disease (Table 4)<sup>[79]</sup>. In primary cultured mouse cortical neurons, KM and PYR were found to be highly neurotoxic, with LC<sub>50</sub> in the low micromolar and nanomolar levels, respectively<sup>[80]</sup>. Further study showed that they could cause a rapid rise in intracellular calcium and strong depolarization of mitochondrial membrane potential. KM- and PYR-induced cell death was reversed by the calcium channel blockers MK-801 and verapamil, suggesting that calcium entry through NMDA receptors and voltage-operated calcium channels are involved in KM- and PYR-induced neurotoxicity. Studies in mice revealed that AZO transferred from the mother to the offspring during gestation by crossing the placenta and entered the developing brain, and high levels of cytotoxicity were observed in embryonic mouse cortical neurons<sup>[29]</sup>.

## Environment transformation

The primary pathways, core mechanism, compound-specific behaviors and key drivers for both abiotic and biotic transformation of the SFs are illustrated in Fig. 3. The detailed discussion is shown below.

## Abiotic transformation

Abiotic transformation of SFs involves multiple metabolic pathways based on their molecular structure. These pathways include the formation of free acrylic acid through the hydrolysis of methyl esters, aromatic cyclohydroxylation, and conjugation with glutathione or other biological groups. Additionally, the double bonds in the acrylic moiety can undergo epoxidation, forming carboxyl groups or alcohols through the addition of hydrogen or water<sup>[83]</sup>. In aquatic environments, KM is particularly prone to forming acidic metabolites, influenced significantly by abiotic factors such as pH, temperature, light, and atmospheric CO<sub>2</sub> levels<sup>[4]</sup>. Photoconversion of AZO is expected to occur through several parallel reaction pathways, including photoisomerization (E/Z), photohydrolysis of methyl and nitrile groups, cleavage of acrylate double bonds, and cleavage of photohydrolytic ethers between aromatic rings to yield phenols. Furthermore, oxidative cleavage of acrylate double bonds is also observed<sup>[83]</sup>. Under field conditions, photolysis is the primary degradation pathway for TRI, with the duration of sunlight exposure being a critical factor<sup>[84]</sup>. In contrast, PYR undergoes rapid transformation under conditions of humid air, with the organic matter content, microbial population, and soil moisture serving as the primary influencing factors<sup>[6]</sup>. Meanwhile, MAND, which features a unique methoxyacetamide functional group, exhibits resistance to alkaline hydrolysis, similar to mandestrobin, which also possesses this methoxyacetamide moiety and shows comparable resistance<sup>[85]</sup>. We further compared the half-lives of these SFs across different environmental matrices. In aquatic systems, MAND demonstrated the shortest photolytic half-life (1.2–3 d) under light exposure, followed by KM with an aqueous half-life of 5.2 d. AZO exhibited the longest persistence in water with a half-life of 15 d. For soil environments, TRI and PYR showed comparable photolysis half-lives of 8.8 and 9.2 d, respectively.

## Biotransformation

Microbial degradation stands out as the primary biotransformation pathway for SFs, with specific soil microorganisms utilizing these chemicals as carbon sources. Notably, four species, *Stenotrophomonas maltophilia*, *Bacillus amyloliquefaciens*, *Bacillus flexus*, and *Arthrobacter oxydans*, are known to metabolize TRI for carbon<sup>[86]</sup>. These species were isolated through a sequential soil and liquid culture enrichment technique. Additionally, two strains, *Cupriavidus* sp. CCH2 and *Rhodanobacter* sp. CCH1, have been isolated for their ability to use AZO as their exclusive carbon and nitrogen source, and they can also degrade TRI, PYR, and KM when additional carbon is available<sup>[87,88]</sup>. Significant differences in the degradation rates of SFs were observed

**Table 4** Human related toxicity studies of strobilurin fungicides

Target SFs	Research content	Conclusion	Ref.
PYR	Investigated the toxicological risks of PYR toward HepG2 cells and the mechanisms of intoxication <i>in vitro</i> .	PYR induced DNA damage and mitochondrial dysfunction, leading to excessive generation of intracellular ROS, which ultimately resulted in mitochondrial-mediated cell apoptosis and toxic effects on human hepatocarcinoma HepG2 cells.	[81]
PYR, TRI, FA, FE	Identified transcriptomic signatures shared with neurological disorders by exposing mouse cortical neuron-enriched cultures to PYR, TRI, FA, and FE.	PYR, TRI, FA, and FE induced transcriptional changes <i>in vitro</i> . By inhibiting mitochondrial complex III, and they upregulated <i>Nrf2</i> -targeted antioxidant response genes and <i>Rest</i> . These changes are associated with human brain aging and neurodegeneration.	[79]
TRI	Explored the mechanism of TRI-mediated mitophagy in human skin keratinocytes exposed to TRI.	Mitochondrial damage and mitophagy likely contribute to TRI-induced toxicity in human keratinocytes, suggesting a potential mechanism for cutaneous diseases developed upon exposure.	[70]
AZO	Explored the effects of AZO on human esophageal squamous cell carcinoma KYSE-150 cells and investigated the underlying mechanisms.	AZO effectively induced apoptosis in esophageal cancer cells via mitochondrial-mediated apoptotic pathways.	[72]
PYR	Using a multi-analytical approach that integrates toxicological database mining, protein-protein interaction (PPI) network analysis, and molecular docking, we studied the molecular mechanisms of PYR toxicity.	PYR exposure was significantly associated with pathways related to prostate cancer and renal dysfunction, indicating its potential role as an inducer of these diseases.	[82]



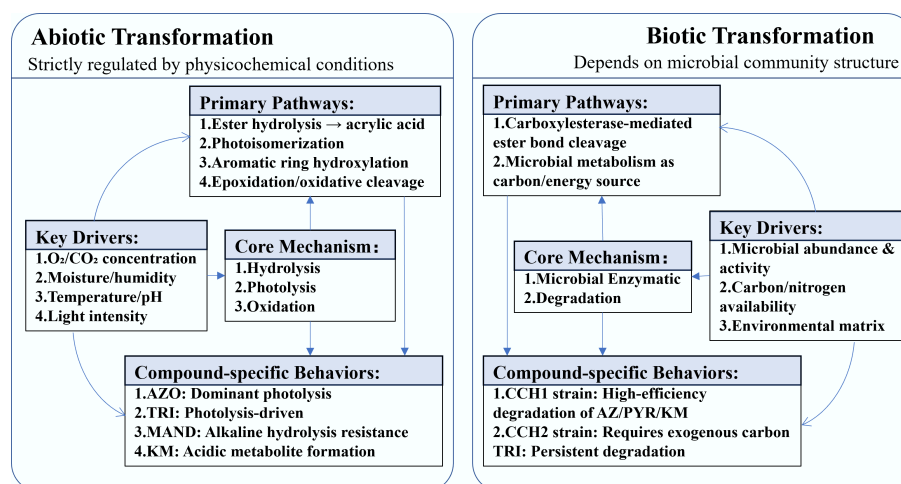


**Fig. 3** Comparison of abiotic vs biotic transformation pathways for strobilurin fungicides.

between microbial strains. Specifically, CCH1 demonstrated universally higher degradation efficiency than CCH2 for three strobilurins—AZ (DT25: 2.0 d vs 2.2 d), PYR (2.3 d vs 2.8 d), and KM (2.6 d vs 2.9 d)—with the most pronounced disparity occurring in PYR degradation. Additionally, TRI exhibited the slowest degradation across both strains (identical DT25 of 4.2 d), markedly exceeding other SFs. Other studies have shown that HI2 and HI6 achieved a PYR degradation rate of  $0.1 \text{ mg} \cdot (\text{L} \cdot \text{d})^{-1}$ .

While SFs have a complex structure with numerous active sites, the underlying molecular mechanisms of their biodegradation are consistent across different species. Carboxylester hydrolysis by esterases is often the primary degradation mechanism in the microbial-guided biotransformation of strobilurins. This enzymatic process effectively cleaves the ester bonds within the molecules, initiating degradation and enabling further metabolic transformations<sup>[12,88,89]</sup>.

## Research gaps and recommendations

The widespread presence of SFs in environmental media, foodstuffs, and human populations suggests a large-scale and potentially global contamination trend. Human exposure to SFs occurs through various pathways that have been established for other pesticides, including oral ingestion, dermal absorption, hand-to-mouth transfer, and additional mechanisms. To date, human biomonitoring studies remain limited, and Tolerable Daily Intake (TDI) values are generally lacking for SFs. Available research indicates that SFs exhibit toxicity not only to aquatic species but also to mammals, including humans. However, the existing data are insufficient for a comprehensive assessment of human exposure routes and associated risks for SFs. Further research is necessary across multiple domains, including environmental monitoring, toxicological effects, biomonitoring, and human exposure assessments. Knowledge gaps have been identified and prioritized to the best of our current understanding to guide future research endeavors.

### Enhancing environmental monitoring and exposure assessment

Despite the widespread use of SFs, critical gaps persist in characterizing their environmental distribution. Comprehensive monitoring across matrices such as air, indoor/outdoor dust, drinking water, and

consumer products remains limited. Large-scale regional and global studies are urgently needed to establish baseline concentrations and evaluate the spatial-temporal dynamics of these emerging contaminants. Concurrently, exposure pathways—including dietary and non-dietary routes—must be systematically quantified, particularly for sensitive populations (e.g., children, pregnant women). Advanced analytical frameworks integrating source tracking, fate modeling, and biomonitoring are essential to refine risk assessments and inform regulatory policies.

### Advancing mechanistic toxicity studies

While mitochondrial dysfunction has been identified as a primary toxicity endpoint for SFs in mammals, the molecular mechanisms driving these effects remain poorly understood. Current research disproportionately focuses on mitochondrial endpoints, neglecting potential interactions with other cellular pathways (e.g., epigenetic regulation, immune disruption). Cutting-edge omics technologies (e.g., transcriptomics, metabolomics, proteomics) should be prioritized to unravel systemic toxicity profiles and identify novel biomarkers of effect. Furthermore, investigations into mixture toxicity and cumulative effects are critical, given the co-occurrence of SFs with other agrochemicals in environmental matrices.

### Expanding epidemiological evidence

Epidemiological data linking SFs exposure to human health outcomes are strikingly scarce. Robust cohort studies incorporating biomonitoring (e.g., urine, blood SF metabolites) and longitudinal health assessments are imperative to evaluate associations with chronic diseases, developmental anomalies, and endocrine disorders. Special attention should be directed toward agricultural communities and regions with intensive SF usage, where exposure levels are likely elevated. Harmonized methodologies for exposure quantification and outcome measurement are needed to ensure comparability across studies.

### Leveraging predictive effect modeling

Empirical testing of SF toxicity across all ecologically relevant species—particularly under realistic exposure scenarios involving mixtures and environmental stressors—is logistically unfeasible. Effect modeling offers a transformative alternative:

Toxicokinetic-Toxicodynamic (TK-TD) Models: proven frameworks for predicting time-dependent toxicity under variable exposure regimes<sup>[90,91]</sup>, such as those based on acute mortality data, should be expanded to sublethal endpoints (e.g., growth inhibition, reproductive impairment).

Quantitative Structure-Toxicity Relationship (QSTR) Models: existing multi-species QSTR models, which accurately predict SFs toxicity across 20 indicator species (invertebrates and vertebrates), warrant validation in field conditions and extension to underrepresented taxa<sup>[92,93]</sup>.

Mixture Toxicity Modeling: integrate chemical interaction algorithms (e.g., concentration addition, independent action) to assess cumulative risks of SFs co-exposures<sup>[90]</sup>.

## Author contributions

study conception and design, authorship team assembling, writing – draft manuscript preparation: Xue J, Liu Z, Liu Y; metadata compiling and analysis: Liu Z, Liu Y; writing – manuscript editing: Zhang H, Zhao Y, Zhang T, Cai Y. All authors commented on the draft and gave final consent for publication.

## Data availability

The datasets generated during and/or analyzed in the current study are available from the corresponding author on reasonable request.

## Funding

This work was supported by the Basic Science Center Project of the Natural Science Foundation of China (52388101), the Program for Guangdong Introducing Innovative and Entrepreneurial Teams (2019ZT08L213), the Natural Science Foundation of China (42377376), the Guangdong Provincial Key Laboratory Project (2023B1212060068), and the R & D program of Guangdong Provincial Department of Science and Technology (2024B1212040004).

## Declarations

### Competing interests

The authors declare that they have no known competing financial interests or personal relationships that could have influenced the work reported in this paper.

### Author details

<sup>1</sup>Guangdong Basic Research Center of Excellence for Ecological Security and Green Development, Key Laboratory for City Cluster Environmental Safety and Green Development of the Ministry of Education, School of Ecology, Environment and Resources, Guangdong University of Technology, Guangzhou 510006, China; <sup>2</sup>Guangdong Provincial Key Laboratory of Water Quality Improvement and Ecological Restoration for Watersheds, Institute of Environmental and Ecological Engineering, Guangdong University of Technology, Guangzhou 510006, China; <sup>3</sup>Guangdong Provincial Observation and Research Station for Social-Natural Complex Ecosystems in Haizhu Wetlands, Guangzhou 510006, China; <sup>4</sup>Key Laboratory of Ministry of Education for Water Quality Security and Protection in Pearl River Delta, School of Environmental Science and Engineering, Guangzhou University, Guangzhou 510006, China; <sup>5</sup>School of Agriculture and Biotechnology, Sun Yat-Sen University, Shenzhen 518107, China

## References

- [1] Anke T, Oberwinkler F, Steglich W, Schramm G. 1977. The strobilurins—new antifungal antibiotics from the basidiomycete *Strobilurus tenacellus*. *The Journal of Antibiotics* 30:806–810
- [2] Bartlett DW, Clough JM, Godwin JR, Hall AA, Hamer M, Parr-Dobrzanski B. 2002. The strobilurin fungicides. *Pest Management Science* 58:649–662
- [3] Bartlett DW, John M. Clough, Chris R. A. Godfrey, Jeremy R. Godwin, Alison A. Hall, et al. 2001. Understanding the strobilurin fungicides. *Pesticide Outlook* 12:143–148
- [4] Khandelwal A, Gupta S, Gajbhiye VT, Varghese E. 2014. Degradation of kresoxim-methyl in soil: Impact of varying moisture, organic matter, soil sterilization, soil type, light and atmospheric CO<sub>2</sub> level. *Chemosphere* 111:209–217
- [5] Rodrigues ET, Lopes I, Pardal MÂ. 2013. Occurrence, fate and effects of azoxystrobin in aquatic ecosystems: A review. *Environment International* 53:18–28
- [6] Feng Y, Huang Y, Zhan H, Bhatt P, Chen S. 2020. An overview of strobilurin fungicide degradation: current status and future perspective. *Frontiers in Microbiology* 11:1–11
- [7] Wang K, Sun Z, Yang L, He L, Li X, et al. 2020. Respiratory toxicity of azoxystrobin, pyraclostrobin and coumoxystrobin on *Chlorella vulgaris*. *Bulletin of Environmental Contamination and Toxicology* 104:799–803
- [8] Wang X, Li X, Wang Y, Qin Y, Yan B, et al. 2021. A comprehensive review of strobilurin fungicide toxicity in aquatic species: emphasis on mode of action from the zebrafish model. *Environmental Pollution* 275:116671–116683
- [9] Kumar N, Willis A, Satbhai K, Ramalingam L, Schmitt C, et al. 2020. Developmental toxicity in embryo-larval zebrafish (*Danio rerio*) exposed to strobilurin fungicides (azoxystrobin and pyraclostrobin). *Chemosphere* 241:124980
- [10] Shin HM, Moschet C, Young TM, Bennett DH. 2019. Measured concentrations of consumer product chemicals in California house dust: Implications for sources, exposure, and toxicity potential. *Indoor Air* 30:60–75
- [11] Cooper EM, Rushing R, Hoffman K, Phillips AL, Hammel SC, et al. 2020. Strobilurin fungicides in house dust: is wallboard a source? *Journal of Exposure Science & Environmental Epidemiology* 30:247–252
- [12] Balba H. 2007. Review of strobilurin fungicide chemicals. *Journal of Environmental Science and Health, Part B* 42:441–451
- [13] Kim JH, Campbell BC, Mahoney N, Chan KL, Molyneux RJ, et al. 2007. Enhanced activity of strobilurin and fludioxonil by using berberine and phenolic compounds to target fungal antioxidative stress response. *Letters in Applied Microbiology* 45:134–141
- [14] Wania F. 2003. Assessing the potential of persistent organic chemicals for long-range transport and accumulation in polar regions. *Environmental Science & Technology* 27:1344–1351
- [15] Kelly BC, Ikonomou MG, Blair JD, Morin AE, Gobas FAPC. 2007. Food web-specific biomagnification of persistent organic pollutants. *Science* 317:236–239
- [16] Zhang C, Zhou T, Xu Y, Du Z, Li B, et al. 2020. Ecotoxicology of strobilurin fungicides. *Science of the Total Environment* 742:140611–140623
- [17] Mohapatra S, Siddamalliah L, Matadha NY. 2021. Behavior of acetamiprid, azoxystrobin, pyraclostrobin, and lambda-cyhalothrin in/on pomegranate tissues. *Environmental Science and Pollution Research* 28:27481–27492
- [18] He L, He F, Yang S, Gao Y, Li B, et al. 2021. Dissipation kinetics and safety evaluation of pyraclostrobin and its desmethoxy metabolite BF 500-3 in a cucumber greenhouse agroecosystem. *Environmental Science and Pollution Research* 28:17712–17723
- [19] Gomes HdO, Cardoso RdS, da Costa JGM, Andrade da Silva VP, Nobre CdA, et al. 2021. Statistical evaluation of analytical curves for quantification of pesticides in bananas. *Food Chemistry* 345:128768
- [20] Li P, Sun P, Dong X, Li B. 2020. Residue analysis and kinetics modeling of thiophanate-methyl, carbendazim, tebuconazole and pyraclostrobin in apple tree bark using Q/ECHERS/HPLC-VWD. *Biomedical Chromatography* 34:e4851
- [21] Gao Y, Yang S, Li X, He L, Zhu J, et al. 2019. Residue determination of pyraclostrobin, picoxystrobin and its metabolite in pepper fruit via

- UPLC-MS/MS under open field conditions. *Ecotoxicology and Environmental Safety* 182:109445–109453
- [22] Paramasivam M, Deepa M, Selvi C, Chandrasekaran S. 2017. Dissipation kinetics and safety evaluation of tebuconazole and trifloxystrobin in tea under tropical field conditions. *Food Additives & Contaminants: Part A* 34:2155–2163
- [23] Kang D, Zhang H, Chen Y, Wang F, Shi L, et al. 2017. Simultaneous determination of difenoconazole, trifloxystrobin and its metabolite trifloxystrobin acid residues in watermelon under field conditions by GC-MS/MS. *Biomedical Chromatography* 31:e3987
- [24] Peng W, Zhao L, Liu F, Xue J, Li H, et al. 2014. Effect of paste processing on residue levels of imidacloprid, pyraclostrobin, azoxystrobin and fipronil in winter jujube. *Food Additives & Contaminants: Part A* 31:1562–1567
- [25] Li X, Li B, Chen M, Yan M, Cao X, et al. 2021. Preparation of magnetic zeolitic imidazolate framework-8 for magnetic solid-phase extraction of strobilurin fungicides from environmental water samples. *Analytical Methods* 13:2943–2950
- [26] Li H, Yang S, Li T, Li X, Huang X, et al. 2020. Determination of pyraclostrobin dynamic residual distribution in tilapia tissues by UPLC-MS/MS under acute toxicity conditions. *Ecotoxicology and Environmental Safety* 206:111182
- [27] Yusa V, Millet M, Coscolla C, Roca M. 2015. Analytical methods for human biomonitoring of pesticides. *A review. Analytica Chimica Acta* 891:15–31
- [28] Gallo V, Tomai P, Gherardi M, Fanali C, De Gara L, et al. 2021. Dispersive liquid-liquid microextraction using a low transition temperature mixture and liquid chromatography-mass spectrometry analysis of pesticides in urine samples. *Journal of Chromatography A* 1642:462036
- [29] Hu W, Liu CW, Jiménez JA, McCoy ES, Hsiao YC, et al. 2022. Detection of azoxystrobin fungicide and metabolite azoxystrobin-acid in pregnant women and children, estimation of daily intake, and evaluation of placental and lactational transfer in mice. *Environmental Health Perspectives* 130:027013–027022
- [30] Chang C, Chen M, Gao J, Luo J, Wu K, et al. 2017. Current pesticide profiles in blood serum of adults in Jiangsu Province of China and a comparison with other countries. *Environment International* 102:213–222
- [31] Flores JL, Díaz AM, Fernández de Córdova ML. 2007. Determination of azoxystrobin residues in grapes, musts and wines with a multicommuted flow-through optosensor implemented with photochemically induced fluorescence. *Analytica Chimica Acta* 585:185–191
- [32] Guo X, Wang K, Chen GH, Shi J, Wu X, et al. 2017. Determination of strobilurin fungicide residues in fruits and vegetables by nonaqueous micellar electrokinetic capillary chromatography with indirect laser-induced fluorescence. *Electrophoresis* 38:2004–2010
- [33] Kolosova A, Maximova K, Eremin SA, Zherdev AV, Mercader JV, et al. 2017. Fluorescence polarisation immunoassays for strobilurin fungicides kresoxim-methyl, trifloxystrobin and picoxystrobin. *Talanta: The International Journal of Pure and Applied Analytical Chemistry* 162:495–504
- [34] Nogueira FdS, Araujo FM, De Faria LV, Lisboa TP, Azevedo GC, et al. 2020. Simultaneous determination of strobilurin fungicides residues in bean samples by HPLC-UV-AD using boron-doped diamond electrode. *Talanta* 216:120957
- [35] Kwon CH, Lee YD, Im MH. 2011. Simultaneous determination of oryzastron and its isomers in rice using HPLC-UV and LC-MS/MS. *Journal of Agricultural and Food Chemistry* 59:10826–10830
- [36] Christensen HB, Granby K. 2001. Method validation for strobilurin fungicides in cereals and fruit. *Food Additives & Contaminants* 18:866–874
- [37] Liu C, Qin D, Zhao Y, Pan C, Jiang S, et al. 2010. Famoxadone residue and dissipation in watermelon and soil. *Ecotoxicology and Environmental Safety* 73:183–188
- [38] Abdelraheem EMH, Hassan SM, Arief MMH, Mohammad SG. 2015. Validation of quantitative method for azoxystrobin residues in green beans and peas. *Food Chemistry* 182:246–250
- [39] Jia L, Huang X, Zhao W, Wang H, Jing X. 2020. An effervescence tablet-assisted microextraction based on the solidification of deep eutectic solvents for the determination of strobilurin fungicides in water, juice, wine, and vinegar samples by HPLC. *Food Chemistry* 317:126424
- [40] Luo X, Qin X, Liu Z, Chen D, Yu W, et al. 2020. Determination, residue and risk assessment of trifloxystrobin, trifloxystrobin acid and tebuconazole in Chinese rice consumption. *Biomedical Chromatography* 34:e4694
- [41] Huang X, Du Z, Wu B, Jia L, Wang X, et al. 2020. Dispersive liquid-liquid microextraction based on the solidification of floating organic droplets for HPLC determination of three strobilurin fungicides in cereals. *Food Additives & Contaminants: Part A* 37:1279–1288
- [42] Xue J, Li H, Liu F, Jiang W, Chen X. 2014. Determination of strobilurin fungicides in cotton seed by combination of acetonitrile extraction and dispersive liquid-liquid microextraction coupled with gas chromatography. *Journal of Separation Science* 37:845–852
- [43] de Melo Abreu S, Caboni P, Cabras P, Garau VL, Alves A. 2006. Validation and global uncertainty of a liquid chromatographic with diode array detection method for the screening of azoxystrobin, kresoxim-methyl, trifloxystrobin, famoxadone, pyraclostrobin and fenamidone in grapes and wine. *Analytica Chimica Acta* 573-574:291–297
- [44] López-Ruiz R, Romero-González R, Garrido Frenich A. 2019. Residues and dissipation kinetics of famoxadone and its metabolites in environmental water and soil samples under different conditions. *Environmental Pollution* 252:163–170
- [45] Raina-Fulton R. 2015. Determination of neonicotinoid insecticides and strobilurin fungicides in particle phase atmospheric samples by liquid chromatography-tandem mass spectrometry. *Journal of Agricultural and Food Chemistry* 63:5152–5162
- [46] Liu J, Wan Y, Jiang Y, Xia W, He Z, et al. 2022. Occurrence of azole and strobilurin fungicides in indoor dust from three cities of China. *Environmental Pollution* 304:119168
- [47] Zubrod JP, Bundschuh M, Arts G, Brühl CA, Imfeld G, et al. 2019. Fungicides: an overlooked pesticide class? *Environmental Science & Technology* 53:3347–3365
- [48] Berenzen N, Lentzen-Godding A, Probst M, Schulz H, Schulz R, et al. 2005. A comparison of predicted and measured levels of runoff-related pesticide concentrations in small lowland streams on a landscape level. *Chemosphere* 58:683–691
- [49] Reilly TJ, Smalling KL, Orlando JL, Kuivila KM. 2012. Occurrence of boscalid and other selected fungicides in surface water and groundwater in three targeted use areas in the United States. *Chemosphere* 89:228–234
- [50] Liu J, Xia W, Wan Y, Xu S. 2021. Azole and strobilurin fungicides in source, treated, and tap water from Wuhan, central China: Assessment of human exposure potential. *Science of the Total Environment* 801:149733
- [51] Zhao Z, Sun R, Su Y, Hu J, Liu X. 2021. Fate, residues and dietary risk assessment of the fungicides epoxiconazole and pyraclostrobin in wheat in twelve different regions, China. *Ecotoxicology and Environmental Safety* 207:111236
- [52] Hou Z, Wang X, Zhao X, Wang X, Yuan X, et al. 2016. Dissipation rates and residues of fungicide azoxystrobin in ginseng and soil at two different cultivated regions in China. *Environmental Monitoring and Assessment* 188:440
- [53] Hao F, Wang X, Ma F, Wang R, Dong F, et al. 2024. Transfer of pesticides and metabolites in corn: Production, processing, and livestock dietary burden. *Science of the Total Environment* 955:176932
- [54] Wang B, Shi L, Ren P, Qin S, Li J, et al. 2024. Dissipation and dietary risk assessment of the fungicide pyraclostrobin in apples using ultra-high performance liquid chromatography-mass spectrometry. *Molecules* 29:4434–4444
- [55] Dost K, Öksüz M, Citan M, Mutlu B, Tural B. 2023. Determination of boscalid, pyraclostrobin and trifloxystrobin in dried grape and apricot by HPLC/UV method. *Journal of Food Composition and Analysis* 115:104926
- [56] Braun G, Sebesvari Z, Braun M, Kruse J, Amelung W, et al. 2018. Does sea-dyke construction affect the spatial distribution of pesticides in agricultural soils? – A case study from the Red River Delta, Vietnam. *Environmental Pollution* 243:890–899
- [57] Chau ND, Sebesvari Z, Amelung W, Renaud FG. 2015. Pesticide pollution of multiple drinking water sources in the Mekong Delta, Vietnam: evidence from two provinces. *Environmental Science and Pollution Research* 22:9042–9058
- [58] Battaglin WA, Sandstrom MW, Kuivila KM, Kolpin DW, Meyer MT. 2010. Occurrence of azoxystrobin, propiconazole, and selected other



- fungicides in US streams, 2005–2006. *Water, Air, & Soil Pollution* 218:307–322
- [59] Wang Y, Wan Y, Li S, He Z, Xu S, et al. 2023. Occurrence, spatial variation, seasonal difference, and risk assessment of neonicotinoid insecticides, selected agriculture fungicides, and their transformation products in the Yangtze River, China: From the upper to lower reaches. *Water Research* 247:120724
- [60] Jamin EL, Bonvallot N, Tremblay-Franco M, Cravedi JP, Chevrier C, et al. 2014. Untargeted profiling of pesticide metabolites by LC-HRMS: an exposomics tool for human exposure evaluation. *Analytical & Bioanalytical Chemistry* 406:1149
- [61] Perez-Rodriguez V, Wu N, de la Cova A, Schmidt J, Denslow ND, Martyniuk CJ. 2020. The organochlorine pesticide toxaphene reduces non-mitochondrial respiration and induces heat shock protein 70 expression in early-staged zebrafish (*Danio rerio*). *Comparative Biochemistry and Physiology Part C: Toxicology & Pharmacology* 228:108669
- [62] Yang L, Huang T, Li R, Souders CL, Rheingold S, et al. 2021. Evaluation and comparison of the mitochondrial and developmental toxicity of three strobilurins in zebrafish embryo/larvae. *Environmental Pollution* 270:116277
- [63] Cao F, Wu P, Huang L, Li H, Qian L, et al. 2018. Short-term developmental effects and potential mechanisms of azoxystrobin in larval and adult zebrafish (*Danio rerio*). *Aquatic Toxicology* 198:129–140
- [64] Li H, Zhao F, Cao F, Teng M, Yang Y, et al. 2019. Mitochondrial dysfunction-based cardiotoxicity and neurotoxicity induced by pyraclostrobin in zebrafish larvae. *Environmental Pollution* 251:203–211
- [65] Jiang J, Wu S, Lv L, Liu X, Chen L, et al. 2019. Mitochondrial dysfunction, apoptosis and transcriptomic alterations induced by four strobilurins in zebrafish (*Danio rerio*) early life stages. *Environmental Pollution* 253:722–730
- [66] Huang X, Yang S, Li B, Wang A, Li H, et al. 2021. Comparative toxicity of multiple exposure routes of pyraclostrobin in adult zebrafish (*Danio rerio*). *Science of the Total Environment* 777:145957
- [67] Liu L, Jiang C, Wu ZQ, Gong YX, Wang GX. 2013. Toxic effects of three strobilurins (trifloxystrobin, azoxystrobin and kresoxim-methyl) on mRNA expression and antioxidant enzymes in grass carp (*Ctenopharyngodon idella*) juveniles. *Ecotoxicology and Environmental Safety* 98:297–302
- [68] Gao AH, Fu YY, Zhang KZ, Zhang M, Jiang HW, et al. 2014. Azoxystrobin, a mitochondrial complex III Qo site inhibitor, exerts beneficial metabolic effects in vivo and in vitro. *Biochimica et Biophysica Acta (BBA) - General Subjects* 1840:2212–2221
- [69] Flampouri E, Mavrikou S, Mouzaki-Paxinou AC, Kintzios S. 2016. Alterations of cellular redox homeostasis in cultured fibroblast-like renal cells upon exposure to low doses of cytochrome bc1 complex inhibitor kresoxim-methyl. *Biochemical Pharmacology* 113:97–109
- [70] Jang Y, Kim JE, Jeong SH, Paik MK, Kim JS, et al. 2016. Trifloxystrobin-induced mitophagy through mitochondrial damage in human skin keratinocytes. *The Journal of Toxicological Sciences* 41:731–737
- [71] Chen H, Li L, Lu Y, Shen Y, Zhang M, et al. 2020. Azoxystrobin reduces oral carcinogenesis by suppressing mitochondrial complex III activity and inducing apoptosis. *Cancer Management and Research Volume* 12:11573–11583
- [72] Shi XK, Bian XB, Huang T, Wen B, Zhao L, et al. 2017. Azoxystrobin induces apoptosis of human esophageal squamous cell carcinoma KYSE-150 cells through triggering of the mitochondrial pathway. *Frontiers in Pharmacology* 8:1–11
- [73] Rodrigues ET, Pardal MÂ, Laizé V, Canela ML, Oliveira PJ, et al. 2015. Cardiomyocyte H9c2 cells present a valuable alternative to fish lethal testing for azoxystrobin. *Environmental Pollution* 206:619–626
- [74] Ma J, Cheng C, Du Z, Li B, Wang J, et al. 2019. Toxicological effects of pyraclostrobin on the antioxidant defense system and DNA damage in earthworms (*Eisenia fetida*). *Ecological Indicators* 101:111–116
- [75] Cao F, Li H, Zhao F, Wu P, Qian L, et al. 2019. Parental exposure to azoxystrobin causes developmental effects and disrupts gene expression in F1 embryonic zebrafish (*Danio rerio*). *Science of the Total Environment* 646:595–605
- [76] Zhu L, Wang H, Liu H, Li W. 2015. Effect of trifloxystrobin on hatching, survival, and gene expression of endocrine biomarkers in early life stages of medaka (*Oryzias latipes*). *Environmental Toxicology* 30:648–655
- [77] Cui F, Chai T, Liu X, Wang C. 2017. Toxicity of three strobilurins (kresoxim-methyl, pyraclostrobin, and trifloxystrobin) on *Daphnia magna*. *Environmental Toxicology and Chemistry* 36:182–189
- [78] Wu S, Lei L, Liu M, Song Y, Lu S, et al. 2018. Single and mixture toxicity of strobilurin and SDHI fungicides to *Xenopus tropicalis* embryos. *Ecotoxicology and Environmental Safety* 153:8–15
- [79] Pearson BL, Simon JM, McCoy ES, Salazar G, Fragola G, et al. 2016. Identification of chemicals that mimic transcriptional changes associated with autism, brain aging and neurodegeneration. *Nature Communications* 7:11173
- [80] Regueiro J, Olguín N, Simal-Gándara J, Suñol C. 2015. Toxicity evaluation of new agricultural fungicides in primary cultured cortical neurons. *Environmental Research* 140:37–44
- [81] Wu M, Bian J, Han S, Zhang C, Xu W, et al. 2023. Characterization of hepatotoxic effects induced by pyraclostrobin in human HepG2 cells and zebrafish larvae. *Chemosphere* 340:139732–139742
- [82] Li SS, Tian XD, Song JK, Wu YD, Wang WL, et al. 2025. Network toxicological and molecular docking in investigating the mechanisms of toxicity of agricultural chemical pyraclostrobin. *Ecotoxicology and Environmental Safety* 297:118244–118255
- [83] Boudina A, Emmelin C, Baalouamer A, Paissé O, Chovelon JM. 2007. Photochemical transformation of azoxystrobin in aqueous solutions. *Chemosphere* 68:1280–1288
- [84] Wang C, Wu J, Zhang Y, Wang K, Zhang H. 2014. Field dissipation of trifloxystrobin and its metabolite trifloxystrobin acid in soil and apples. *Environmental Monitoring and Assessment* 187:4100
- [85] Adachi T, Suzuki Y, Nishiyama M, Kodaka R, Fujisawa T, et al. 2018. Photodegradation of strobilurin fungicide mandestrobin in water. *Journal of Agricultural and Food Chemistry* 66:8514–8521
- [86] Lopes FM, Batista KA, Batista GLA, Mitidieri S, Bataus LAM, et al. 2009. Biodegradation of epoxyconazole and piraclostrobin fungicides by *Klebsiella* sp. from soil. *World Journal of Microbiology and Biotechnology* 26:1155–1161
- [87] Chen X, He S, Liang Z, Li QX, Yan H, et al. 2018. Biodegradation of pyraclostrobin by two microbial communities from Hawaiian soils and metabolic mechanism. *Journal of Hazardous Materials* 354:225–230
- [88] Howell CC, Semple KT, Bending GD. 2014. Isolation and characterisation of azoxystrobin degrading bacteria from soil. *Chemosphere* 95:370–378
- [89] Wang L, Zhao J, Delgado-Moreno L, Cheng J, Wang Y, et al. 2018. Degradation and metabolic profiling for benzene kresoxim-methyl using carbon-14 tracing. *Science of the Total Environment* 637:638:1221–1229. <https://doi.org/10.1016/j.scitotenv.2018.05.123>
- [90] Yang L, Zeng J, Gao N, Zhu L, Feng J. 2024. Predicting the metal mixture toxicity with a toxicokinetic–toxicodynamic model considering the time-dependent adverse outcome pathways. *Environmental Science & Technology* 58:3714–3725
- [91] Tan QG, Wang WX. 2012. Two-compartment toxicokinetic–toxicodynamic model to predict metal toxicity in daphnia magna. *Environmental Science & Technology* 46:9709–9715
- [92] Mukherjee RK, Kumar V, Roy K. 2021. Ecotoxicological QSTR and QSTR modeling for the prediction of acute oral toxicity of pesticides against multiple avian species. *Environmental Science & Technology* 56:335–348
- [93] Basant N, Gupta S, Singh KP. 2015. Predicting aquatic toxicities of chemical pesticides in multiple test species using nonlinear QSTR modeling approaches. *Chemosphere* 139:246–255



Copyright: © 2025 by the author(s). Published by Maximum Academic Press, Fayetteville, GA. This article is an open access article distributed under Creative Commons Attribution License (CC BY 4.0), visit <https://creativecommons.org/licenses/by/4.0>.